Karaelmas Fen ve Mühendislik Dergisi
Journal home page: http://fbd.beun.edu.tr

Research Article
Received / Geliş tarihi : 20.12.2016
Accepted / Kabul tarihi : 30.05.2017

Phase and Microstructural Studies of Two Types Commercial Magnesia and Spinel Refractory Raw Materials with Emphasis on Impurities Characterization

Ticari Olarak Kullanılan İki Çeşit Magnezya ve Spinel Refrakter Hammaddelerindeki Safsızlıkların Faz ve Mikroyapı Karakterizasyon Çalışmaları

Aslı Çakır Arianpour

Department of Ceramic, Faculty of Fine Arts and Design, Kastamonu University, Kastamonu, Turkey

Abstract

Mineralogical impurities of the used magnesia and spinel raw materials are kinds of most important factors which strongly effect on different properties of magnesia-spinel refractories such as melt/slag resistance, physical and thermo mechanical behavior. In this research, two types of commercially available fused/sintered magnesia and spinel raw materials were investigated in terms of microstructure and phase composition with emphasis on the impurities characterization. The phase analysis was studied via X-ray diffraction and the microstructure was investigated using scanning electron microscopy and electron back scattered diffraction techniques. X-ray patterns showed that the main phase in both spinels is MA spinel and any other impurity phases are not detected. The EBSD results revealed that the major phase of sintered magnesia is periclase and the grain boundaries were characterized as merwinite and monticellite. In contrast, for fused one, it is found that the phase composition of grains and boundaries are very similar and were characterized as periclase, merwenite and dispersed monticellite.

Keywords: EBSD characterization, Magnesia, Microstructure, Phase evolution, Refractories, Spinel

Öz

Magnezya ve spinel hammaddelerindeki mineralojik safsızlıklar, magnezya-spinel refrakterlerdeki; örneğin eriyik/cüruf direnci, fiziksel ve termo-mekanik gibi farklı özellikleri etkileyen en önemli parametrelerden biridir. Yapılan bu çalışmada, ticari olarak kullanılan iki çeşit fused/sinter magnezya ve spinel hammaddeleri, safsızlıkların karakterizasyonuna ağırlık verilerek mikroyapı ve faz kompozisyonu açısından incelenmiştir. X-ışınları kırınımı tekniği ile faz analizi, taramalı elektron mikroskobu ve geri yansıyan elektron difraksiyonu tekniği ile mikroyapılar incelenmiştir. Her iki spinele yapılan X-ışınları kırınımı tekniği; ana fazların MA-spinel olduğu ve herhangi bir safsızlığın tespit edilmediğini göstermektedir. Sinter magnezyaya yapılan EBSD analiz sonucu, ana fazın periklas, tane sınırlarında ise mervinit ve montisellit fazlarının olduğunu açığa çıkarmıştır. Buna karşın, fused magnezyada tane ve tane sınırlarındaki faz kompozisyonlarının çok benzer olduğu, periklas, mervinit ve dağılmış durumda montisellit fazının olduğu karakterize edilmiştir.

Anahtar Kelimeler: Karakterizasyon, Magnezya, Mikroyapı, Faz miktarları, Bazik refrakterler, Spinel

1. Introduction

Magnesia (MgO) is one of the main raw materials which has lots of applications in refractory industry (Abadi et al. 2002, Alfarado et al. 2000). This mineral is crystalized in NaCl structure; which in it, each Mg^{+2} ion is bounded with six O^{-2} and each O^{-2} is surrounded with Mg^{+2} (Kingrey et al. 1975). This material is normally producing from calcination of diverse types of magnesium salts especially magnesite ($MgCO_3$) ores. There are two main techniques for production of magnesia via calcination processing which are; first, calcination and sintering of natural magnesite ($MgCO_3$) or brucite ($Mg(OH)_2$) (Bhatti et al. 1984) and; second fusion of raw materials with stoichiometry composition (Bilgiç 2001). Typically, high quality magnesia refractory bricks are composed of 98% MgO which have wide ranges of applications in the steel, cement and non-ferrous metal industries. Sort of different chemical parameters have important rules on the properties of magnesia which is producing to use in high quality basic refractories production. Some of these parameters are the amounts of impurity oxides (CaO, Al_2O_3 and Fe_2O_3), CaO/SiO_2 (C/S) ratio, periclase crystallite size and density. The

*Corresponding Author: acakir@kastamonu.edu.tr

Aslı Çakır Arianpour orcid.org/0000-0002-4050-708X

MgO/impurities ratio controls final phases composition of refractory products; when the amounts of impurities are more than 2 wt.%, it results in a reduction of thermo mechanical properties such as refractoriness under load (RUL) or hot modulus of rupture (HMOR) due to the formation of low melting point phases at high working temperatures (Rodríguez et al. 2016). Calcination of magnesite is also depends on the amounts of impurities, C/S ratio and silicate phases content. The presence of low melting silicate phases at the grain boundaries in some cases improves sintering promotion. Also the presence of some impurity ions such as Al^{+3}, Ti^{+4}, Fe^{+3}, Cr^{+3} and Mn^{+2} will decrease the calcination temperature causes by the crystal defects formation (Han et al. 2007). Dead-burnt (sintered) magnesia normally contains impurities such as silica, lime, iron oxide, and alumina. These impurities can easily react with magnesia and form various calcium or calcium/magnesium silicate phases. The C/S ratio essentially controls the phase composition of MgO particles. In general, high CaO contents (C/S >2.8) results in the formation of tricalcium silicate (Ca_3SiO_5) and free CaO phases, whereas high SiO_2 amount (C/S <0.93) forms monticellite ($CaMgSiO_4$) and forsterite (Mg_2SiO_4) silicate-based phases. This parameter also affects the physical, mechanical and especially high temperature mechanical behaviour. When the SiO_2 content increases (low C/S ratio), due to the formation of eutectic phases, the melting temperature of particles will decrease (Braulio et al. 2008).

Magnesium aluminate spinel ($MgAl_2O_4$ or MA) is another important raw material which is used in the production of basic refractories. MA is normally produced by direct reaction of MgO and Al_2O_3 via heat treating (Bilgiç 2001). Three essential methods are used for the production of MA spinel which includes sintering, fusion and firing (Maryasev et al. 2003, Hamzaçebi 1991). Alumina and magnesia as main raw materials are first crushed and then mixing with organic/inorganic binders. After mixing and drying, the mixture is pressed and sintered in a rotary kiln at more than 1600 ^{o}C to be completely densified. The fired product will be finally crushed and sized by screening. The production of fused spinel is based on the mixing of Al_2O_3 and MgO raw materials according to the stoichiometry composition and then melting in electric arc furnace at 2200^{o}C. Dense fused bricks will be grind and screening to produce sized powder. Due to the high melting temperatures of Al_2O_3 and MgO and consequently high energy consumption, it is thought that this route in not cost effective (Maryasev et al. 2003).

In earlier related studies, most of the efforts have been focused on the microstructural and phase changes of magnesia and spinel refractories in the presence of different additives. However, the characterizations of raw materials and impurities were not essentially discussed. The aim of the present research is to study the effect of impurities on the phase and microstructural characteristics of two available commercial magnesia and spinel in both fused and sintered types which are widely used in production of basic refractory bricks in Turkey.

2. Material and Methods

The used raw materials in this research were two types of available commercial magnesia and spinel powder in both fused and sintered forms which were provided from Kümaş Magnesite Industry Company (Kutahya/Turkey). The chemical analysis of raw materials was determined by using X-ray fluorescency technique (XRF Rigaku ZSX Primus model, Japan). The phases' compositions were determined by means of X-ray diffraction method (XRD Rigaku Rint-2200) to find out the existing phases. The XRD patterns were measured in 2θ range of 20-70° and scan rate of 2°/min. Selected raw materials' samples were in aggregate form which were previously cut by means of diamond disc (Metacome, Germany) and then moulded by cold mounting. For SEM and EDX examinations, surfaces were polished by a coarse metal disc which followed by abrasive discs (50 μm polymer disc (~1 min) and then 6 μm (~ 5 minutes), 3 μm (~ 5 minutes) and 1 μm (~ 3 minutes) abrasive papers) and finally diamond suspension for fine polishing.

The polished surface were examined by using scanning electron microscope (SEM, Zeiss Supra 50VP, Germany) equipped with electron backscatter diffraction (EBSD, HKL Technology) and energy-dispersive X-ray spectroscopy (EDS, Oxford Instruments INCA 7430) detectors. The analyses were performed at 20 kV accelerating voltage and 8-10 mm working distance. Back scattered electron (BSE) images were used to indicate the presence and distribution of different phases.

3. Results and Discussion

Chemical composition of used raw materials including fused/sintered spinel and magnesia are shown in Table 1. According to this table, it is clarified that for both fused and sintered spinel the amounts of alumina and magnesium oxide are near to stoichiometry composition. However the impurity content of fused spinel is a little bit higher than that of sintered spinel in terms of CaO and SiO_2. For magnesia raw materials it shows that the fused one has MgO

purity more than 96.5 wt.%, whereas this value for sintered magnesia is around 93 wt.%. The amount of impurities is respectively decreased for fused type magnesia.

Thermal expansion results which were obtained from dilatometery of the sintered and fused spinel samples at different temperatures are given in Table 2. According to these results thermal expansion coefficient of fused spinel is smaller than sintered one. Because of the higher crystallite size of fused spinel in comparison to the sintered one, it is expected that fused spinel shows lower thermal expansion coefficient and consequently better thermal shock resistance against heat changes.

The phase analysis of the fused and sintered spinel samples which were determined via XRD are given in Figure 1. The XRD results show that the main phase in both samples is MA spinel and any other impurity phases are not detected. It should be consider in mind that some low amount (<3 wt.%) impurity phases may not detectable via XRD due to the detecting limitation of technique.

The SEM images of fractured surfaces of sintered and fused spinel samples are presented in Figure 2 (a) and (b). The magnifications of the SEM images for sintered and fused spinel samples were selected differently due to the huge crystallite size of fused spinel (~ 90 μm) in comparison to the sintered one (~ 5 μm).

The BSE image of polished surface of sintered spinel sample is shown in Figure 3 shows the presence of two different phases which are a minor dark grey (a) and a major (matrix phase) grey (b) areas in the microstructure.

The EDS analyses carried out on these 2 areas were shown in Figure 4. According to the SEM/EDS results in Figures 3 and 4 it is clear that while the matrix phase (area b) contain 72.18 wt.% Al_2O_3 and 27.82 wt.% MgO and expected to be MA spinel phase, the dark grey region (area a) as minor phase contains 100 wt.% MgO which is high MgO phase like as periclase.

Figure 5 shows typical BS SEM images of polished surface of sintered magnesia sample at different magnifications. In these images the presence of different phases with distinguished contrasts is also clear. The general EDS analysis of the sample (Figure 6 (a)) proved that the main constitution grain phase is periclase which has the MgO content equal to 97.15 wt.%. Also the amounts of impurity

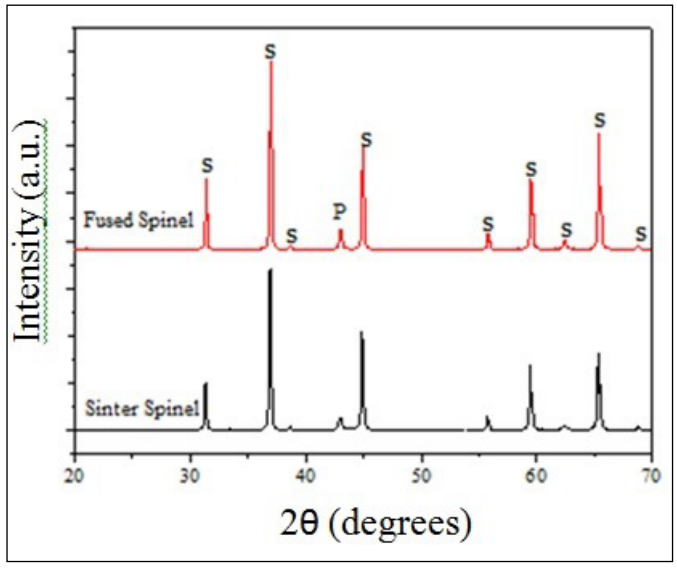

Figure 1. XRD patterns of sintered and fused spinel samples (P: Periclase, S: Spinel).

Table 1. Chemical composition of raw materials.

Sample	MgO	Al_2O_3	SiO_2	CaO	Na_2O	Fe_2O_3	L.O.I.*
Fused Spinel	36.87	61.36	0.37	0.58	0.40	0.21	0.15
Sintered Spinel	35.31	62.77	0.36	0.52	0.39	0.34	0.30
Sintered Magnesia	93.11	0.64	1.32	1.82	2.13	0.46	0.07
Fused Magnesia	96.51	0.14	0.80	1.62	-	0.61	0.20

***L.O.I.**: Loss of Ignition.*

Table 2. Thermal expansion results of fused and sintered spinel samples.

Temperature (°C)	Fused Spinel	Sinter Spinel
	Thermal Expansion (%)	Thermal Expansion (%)
900	0.79	0.80
1000	0.89	0.90
1100	0.99	1.01

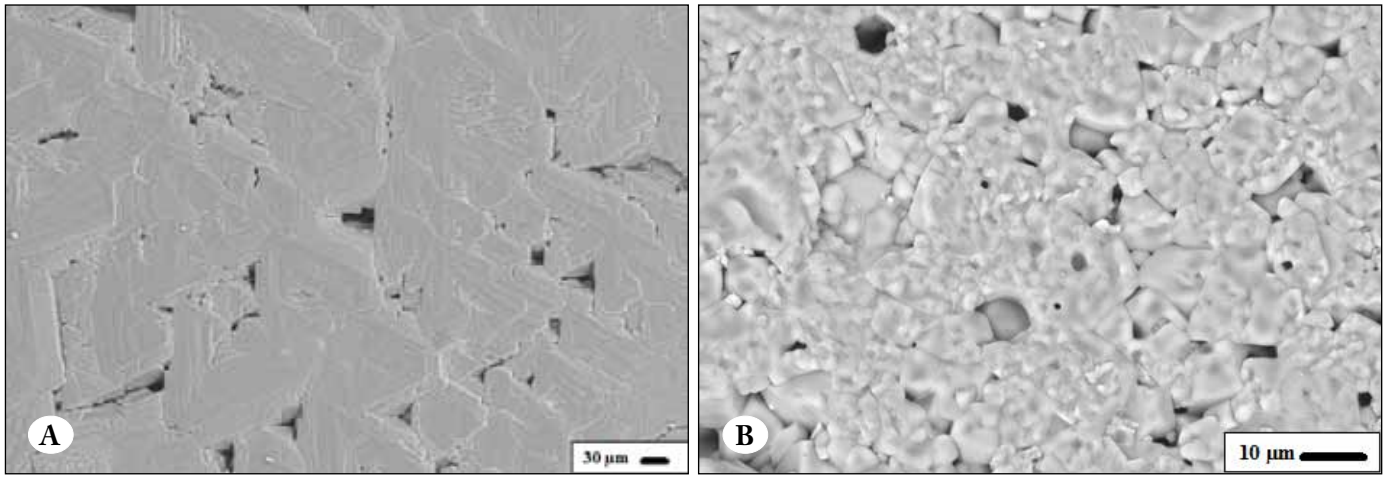

Figure 2. SEM images of the fractured surfaces of **(A)** fused and **(B)** sintered spinel sample.

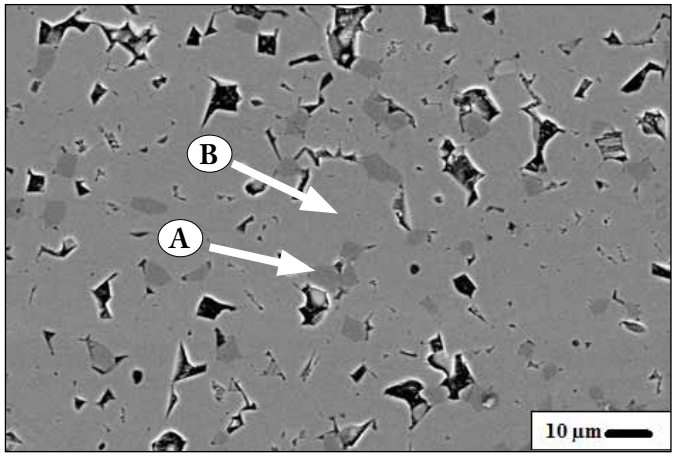

Figure 3. BS SEM image of sintered spinel sample.

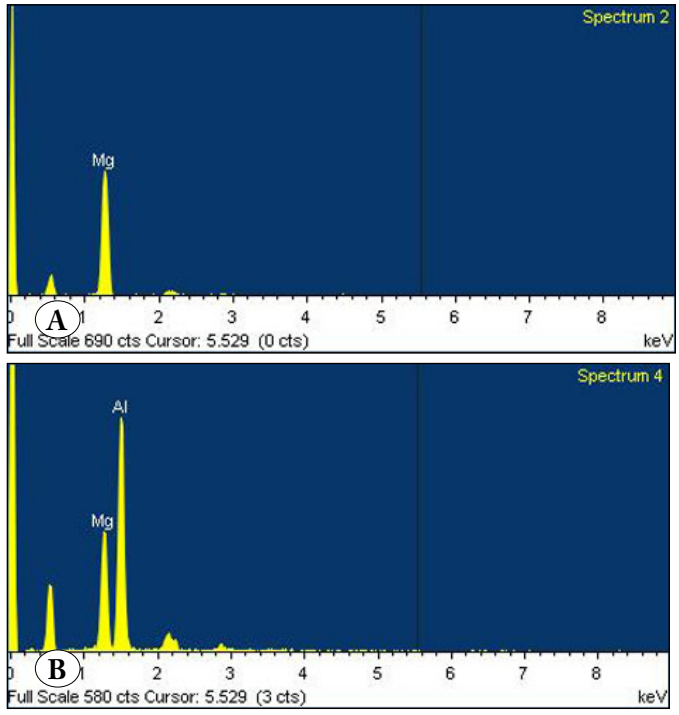

Figure 4. EDS analysis of (a) area a and (b) area b which marked in Figure 3.

oxides in the grains were determined as equal to 1.83 and 1.02 wt.% for CaO and SiO_2, respectively. According to the EDS analysis it is determined that the bright white phase which is presented at the grain boundaries contains 35.94 wt.% SiO_2, 7.56 wt.% MgO and 56.50 wt.% CaO and it is expected that the major constitution phase of grain boundaries is dicalcium silicate ($2CaO.SiO_2$).

One of the most useful characterization techniques which can be applied for investigation of grain and grain boundary phases in refractories' microstructure is electron backscatter diffraction (EBSD) method. Pattern quality mapping technique reveals parts of hidden structural features in texture of materials. This technique clearly shows the surface defects such as grain, grain boundaries and scratches which are not normally visible in the normal structural maps (Ünal 2010). Surface smoothness and quality is one of important affecting parameter in EBSD technique. Figures 7 and 8 show the BS SEM image, quality pattern map, phase map and EBSD phase quantities of sintered and fused magnesia samples .As both these figures show; it is obvious that due to the well applied polishing technique for sample preparation, the quality of surfaces for both samples is excellent which is very important in EBSD technique. As Figure 7 (b) shows, there is a grain boundary phase between grains in the texture of sintered magnesia sample. According to the phase map which is given in Figure 7 (c) it is visible that there are matrix and grain boundary phases in the

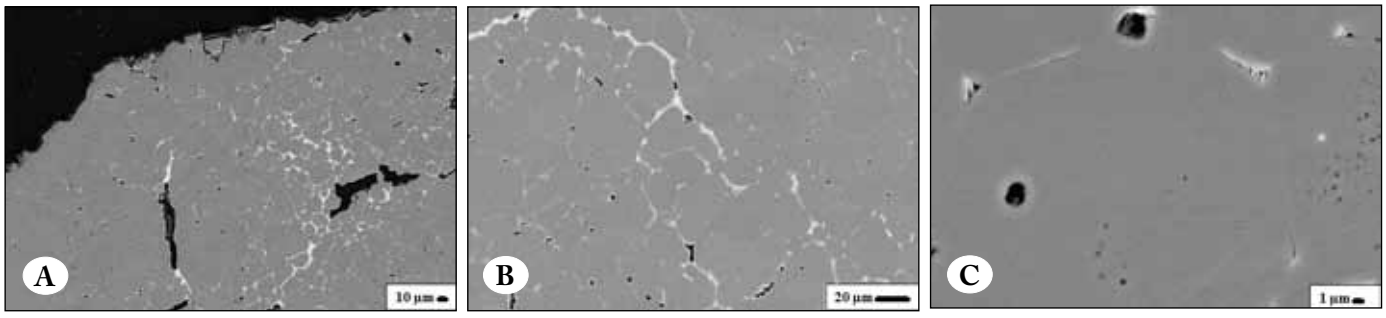

Figure 5. BS SEM images of sintered magnesia sample at **(A)** 500, **(B)** 1000 and **(C)** 2000 X magnifications.

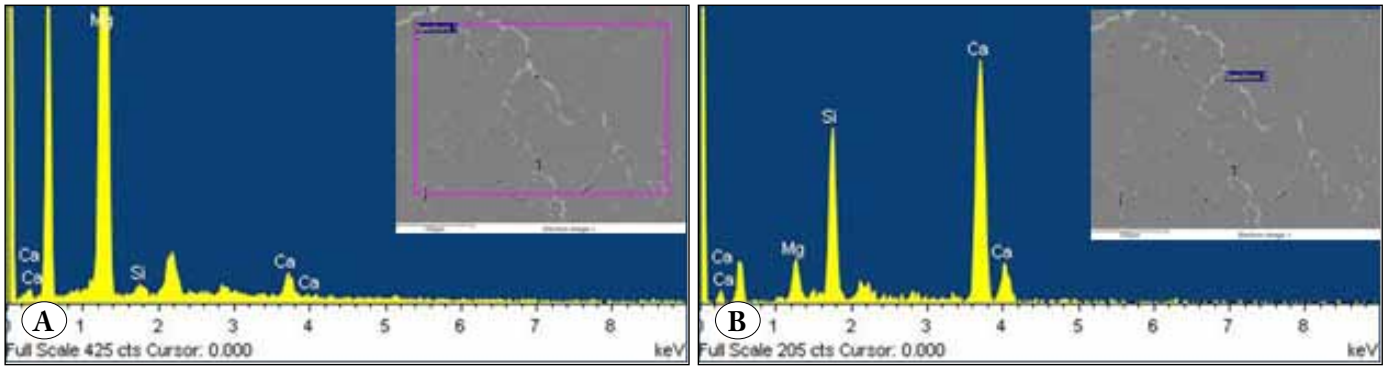

Figure 6. EDS analysis of sintered magnesia sample: **(A)** general surface and **(B)** marked point at grain boundary.

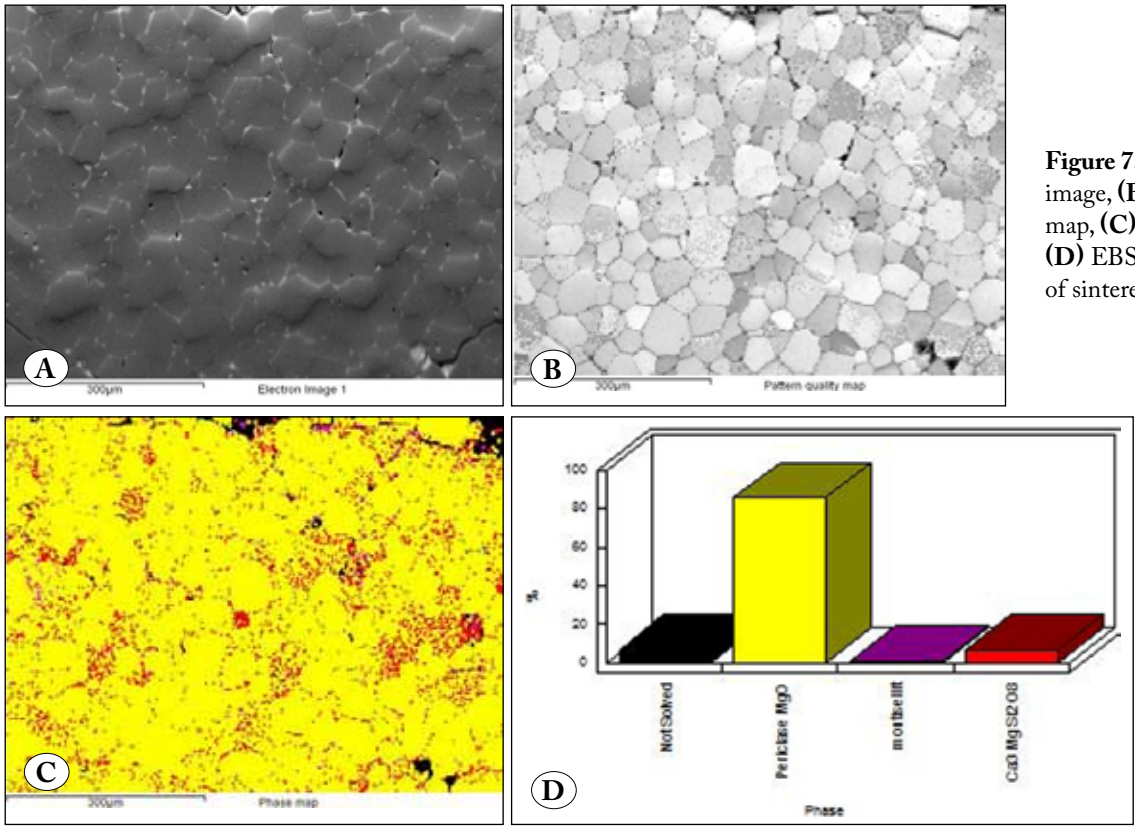

Figure 7. (A) BS SEM image, **(B)** quality pattern map, **(C)** phase map and **(D)** EBSD phase quantities of sintered magnesia sample.

microstructure of this sample. Figure 7 (d) shows the phase composition of this sample in a graph which is derived from EBSD phase quantity technique. It is determined that the major constitution phase of this sample is periclase (85.7 %) which forms the grain phase (matrix) of the sintered magnesia. Also, according to the phase map of this sample (Figure 7 (c)), the presented phases at the grain boundaries were characterized as merwinite ($Ca_3Mg(SiO_4)_2$) and monticellite ($CaMgSiO_4$) which are basically precipitated at the boundaries during cooling period. During the calcination/sintering process of magnesia, the impurity oxides can move from grains toward boundaries and form low melting phases which will be precipitated there. In the quantitative phase graph which is given in Figure 7 (d), the term 'not solved' refers to the not detectable phases (black parts in phase map) which are originated from some surface defect as grain removal during sample preparation.

According to the EBSD results of fused magnesia sample which are given in Figure (8) it is clear that the texture of fused magnesia sample contains large sized grains as matrix phase which is separated with a narrow grain boundaries. Because of the large crystallite size of the fused magnesia due to the high speed crystal growth after melt cooling it is expected that this material has huge sized matrix grains. The main difference between fused and sintered magnesia samples is the texture of matrix and grain boundaries features. In the BS SEM image of this sample, the presence of large periclase grains is clear. Figure 8 (b) shows the quality pattern map of this sample and the presence of grain boundary phase at dark region. Because of the long cracking of the grains and height difference at parts of grain boundaries, some of them were visible as black regions in phase map of Figure 8 (c). This phenomenon leads to detection of some 'unsolved' phase results in the EBSD phase quantitative graph of Figure 8 (d). However, the EBSD technique could successfully characterize the phase constitution of this sample with a good accuracy. As this graph shows, the main constitution phases of matrix grains are periclase (50.8 %) and merwenite (35.3 %) with small amounts of dispersed monticellite (approximately 4 %) in the grains. It should be consider in mind that because of the nature of fusion technique which is consisting of rapid solidification of melt from very high temperatures to room temperature, there is not enough time for separation of impurities from the grain phases to precipitate at the grain boundaries. So, in spite of the sintered magnesia sample,

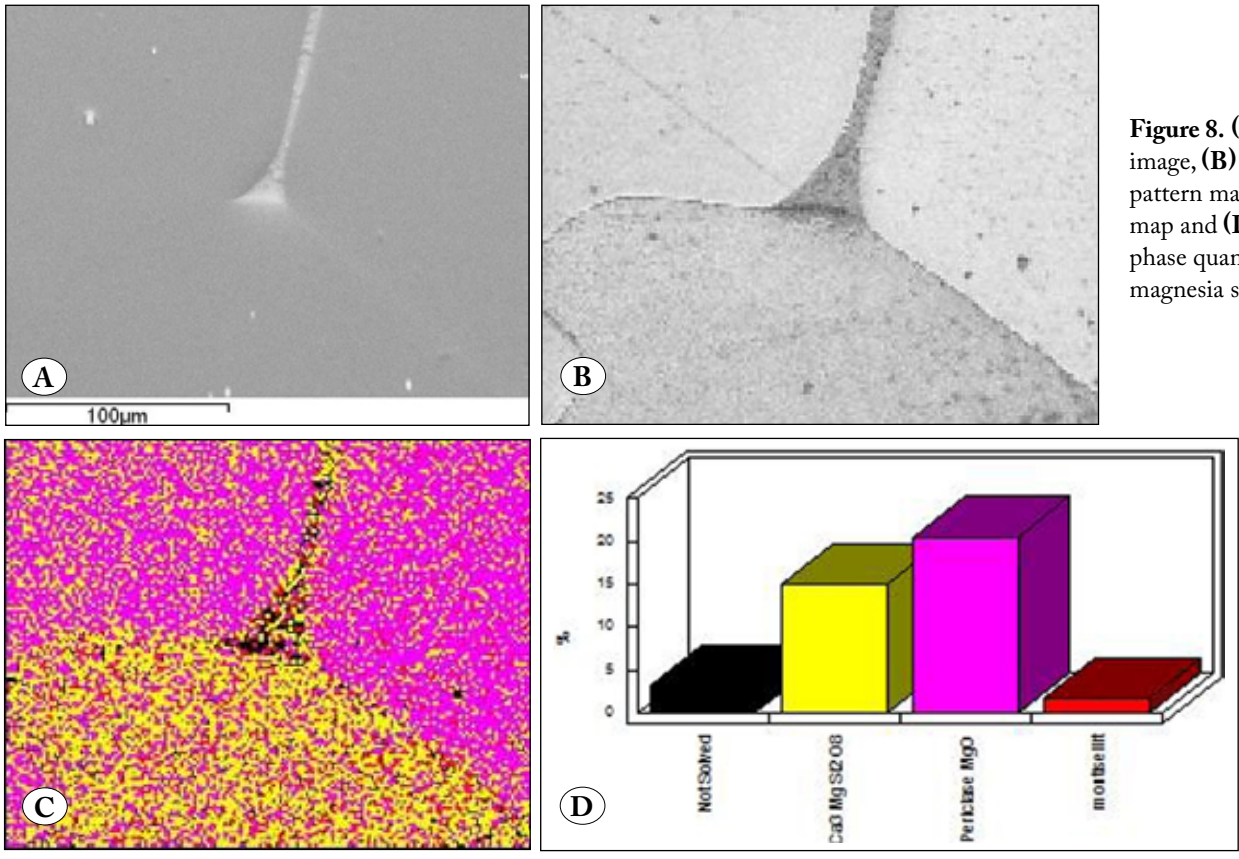

Figure 8. (A) BS SEM image, **(B)** quality pattern map, **(C)** phase map and **(D)** EBSD phase quantities of fused magnesia sample.

the phase composition of grain and boundary phases is very similar for fused magnesia.

4. General Discussions

In this research, two types of commercially available fused/sintered magnesia and spinel raw materials were investigated in terms of microstructure and phase composition with emphasis on the impurities characterization. The phase analysis was studied via X-ray diffraction and the microstructure was investigated using scanning electron microscopy and electron back scattered diffraction techniques. According to XRF results, it is cleared that both fused and sintered spinel samples have the amounts of Al_2O_3 and MgO near to stoichiometry. However the impurity content of fused spinel is a little bit higher than that of sintered one. For magnesia raw materials the amount of impurities of sintered one is higher than that of fused type. Dilatometery results showed that fused spinel has lower thermal expansion coefficient because of the higher crystallite sizes in comparison to the sintered one and expected to have better thermal shock resistance against heat changes. The XRD results showed that the main phase in both spinel samples is MA spinel and any other impurity phases are not detected. The SEM images from fractured surfaces of spinel samples showed the huge crystallite size of fused spinel (~ 90 μm) in comparison to the sintered one (~ 5 μm). Also the BS SEM/EDS image from polished surface of sintered spinel sample showed the presence of two different phases including MA spinel as matrix and periclase as minor phase. The BS SEM/EDS images from polished surface of sintered magnesia proved that the main constitution grain phase is periclase and grain boundaries consist of dicalcium silicate. For in-depth texture and phase composition analysis of magnesia samples, the EBSD technique was utilized. The EBSD result of sintered magnesia revealed that the major constitution phase of this sample is periclase (85.7 %) as grain (matrix) phase. Also, the grain boundaries were characterized as merwinite and monticellite which were precipitated at the boundaries during cooling. The EBSD results of fused magnesia showed that the texture contains of large sized grains as matrix phase which is separated with a narrow grain boundaries. In this sample, the main constitution phases of matrix grains phases were characterized as periclase and merwenite with small amounts of dispersed monticellite. It thought that due to rapid solidification of melt from high melting temperatures to room temperature and insufficient time for impurities' migration from grain to the boundaries, the phase composition of grains and boundaries are very similar for fused magnesia sample.

5. Acknowledgement

The author would like to thank Kümaş Refractory Co. (Kutahya, Turkey) for providing raw materials for this research and also Prof. Dr. Servet Turan, Mrs. Didem Ünal and Mr. Tolun Oğuz for their helps especially EBSD analysis.

6. References

Abadi, E.A.M.H., Golestani, F., and Moztarzadeh, F. 2001. Evaluation of the microstructure of magnesia-zirconia refractories. *Ind. Ceram.*, 22[1]: 19-25.

Alvarado, E., Martinez, M.L., Fuentes, A.F. and Quintana, P. 2000. Preparation and characterization of MgO powders obtained from different magnesium salts and the mineral dolomite, *Polyhedron*, 19: 2345-2351.

Bilgiç, M. 2001. Future of Magnesia and Steelmaking Refractories. *TMMO Metallurgy J.* 127: 43-48.

Bhatti, AS., Dollimore, D., Dyer, A. 1984. Magnesia from seawater: a review. *Clay Min.*, 19: 865-875.

Braulio, M.A.L., Bittencourt, L.R.M. and Pandolfelli, V.C. 2008. Magnesia grain size effect on in situ spinel refractory castables. *J. Eur. Ceramic Soc.,* 28: 2845-2852.

Erdoğan, N, Yıldız, R. 1995. Magnesite and Basic Refractory Material Technology, Lale Publication, Kütahya, 43-44 s.

Hamzaçebi, C. 1991. The Effectes of Process Parameters on the Properties of Spinel Refractories, *Master of Science Thesis*, Istanbul Technical University, 6-8 s.

Han, B., Li, Y., Guo, C., Li, N., Chen, F. 2007. Sintering of MgO-based refractories with added WO_3. *Ceramics Int.*, 33: 1563-1567.

Kingery, WD., Bowen, HK., Uhlmann, DR. 1975. *Introduction to ceramics*, Wiley-InterScience Publication, New York, USA, pp. 61.

Maryasev, G., Koptelov, VN., Kaplan, SF., Koreshkova, MY. 2003. Effect of precursor raw materials on the structure of fused alumina magnesia spinel. *Refrac. Ind. Ceram.*, 44: 405-410.

Rodríguez, E., Moreno, F.H., Aguilar-Martínez, J.A., Montes-Mejía, A.E., Ruiz-Valdés, J.J., Puente-Ornelas, R. and Contreras, J.E. 2016. Effect of nano-titania (η-TiO_2) content on the mechano-physical properties of a magnesia refractory composite. *Ceramics Int.*, 42: 8445-8452.

Ünal, D. 2010. Determination Texture Fraction in Fe-doped Alumina Substrates Used for Production of Carbon. *Master of Sciences Thesis*, Anadolu University, 6 s.